

Stall Flutter Prediction Techniques for Fan and Compressor Blades

V. R. Capece*

University of California, Davis, Davis, California 95616
and

Y. M. EL-Aini†

Pratt and Whitney, United Technologies, West Palm Beach, Florida 33477

A review is presented of stall flutter prediction methodology including empirical, analytical, and semi-empirical approaches. Because of the lack of accurate and efficient unsteady aerodynamic models for stall flutter predictions, interim semiempirical methods are developed to assist turbomachinery designers during the development of current advanced fan and compressor designs for both military and commercial applications. A semiempirical approach that builds on an empirical stall flutter database combined with a classical flat plate linearized unsteady aerodynamic model that accounts for chordwise deformations has been developed. This model is shown to provide good correlations when compared to isolated airfoil and cascade data for standard configurations. When applied to low aspect ratio fans, this approach provided excellent correlations with experimental results.

Nomenclature

| | |
|--------------------------------------|---|
| a, b | = complex constants, Eq. (9) |
| b | = airfoil semichord |
| $C_{\text{experiment}}$ | = experimental lift or moment coefficient magnitude |
| $C_{L, \text{modified}}$ | = modified lift coefficient |
| C_{modified} | = modified lift or moment coefficient |
| $C_{M, \text{modified}}$ | = modified moment coefficient |
| C_{ratio} | = ratio of experimental-to-theoretical lift or moment coefficient magnitude |
| C_{Smith} | = theoretical cascade lift or moment coefficient |
| C_{theory} | = theoretical lift or moment coefficient magnitude |
| h | = translation component at the elastic axis location |
| KE | = average bladed-disk system kinetic energy |
| k | = reduced frequency, $\omega b/U$ |
| NB | = number of blades |
| $q(\xi)$ | = finite element vibratory displacement normal to the airfoil chord |
| $T(\xi)$ | = transfer function |
| U | = inlet relative velocity |
| V | = reduced velocity, $U/b\omega$ |
| W | = unsteady aerodynamic work |
| α | = rotation component around the elastic axis |
| β_{\min} | = flow angle corresponding to minimum loss coefficient |
| β_1 | = airfoil relative inlet flow angle |
| β_{1f} | = normalized incidence |
| β_{1L} | = flow angle at a loss value equal to the minimum loss plus a small increment |
| $\Delta C_{p, \text{modified}}(\xi)$ | = modified pressure difference coefficient |
| $\Delta C_{p, \text{Smith}}$ | = theoretical pressure difference coefficient |

| | |
|------------------------------|--|
| $\Delta\Phi$ | = lift or moment coefficient phase angle for the empirical correction coefficient |
| δ_{aero} | = aerodynamic damping |
| $\delta_{\text{mechanical}}$ | = mechanical damping |
| δ_{total} | = total system damping |
| η | = location of the elastic axis position along the chordline referenced to the leading edge |
| ξ | = distance along the airfoil chord |
| $\Phi_{\text{experiment}}$ | = experimental lift or moment coefficient phase angle |
| Φ_{modified} | = modified lift or moment coefficient phase angle |
| Φ_{Smith} | = theoretical cascade lift or moment phase angle |
| Φ_{theory} | = theoretical lift or moment coefficient phase angle |
| ω | = flutter frequency, rad/s |

Introduction

STALL flutter continues to be a challenging problem for designers of fans and compressors for civilian and military gas turbine engines. As schematically depicted in Fig. 1, stall flutter may occur near the stall line during high-speed operation (supersonic stall flutter), or part-speed operation (subsonic/transonic stall flutter). Because of the close proximity to the stall line, the incidence angles in stall flutter are usually well above the nominal values encountered at the design point, especially for subsonic/transonic stall flutter. Hence, for stall flutter, viscous effects are of significant importance.

Considerable progress has been made in the development of unsteady aerodynamic models for flutter and forced vibrations. However, accurate first-principles prediction of stall flutter still remains elusive. This has resulted because most of the unsteady aerodynamic models developed have been for inviscid flow, with varying degrees of approximation for airfoil geometry. Classical linearization has been used for two-dimensional potential flow over flat plate airfoils to model the unsteady aerodynamics for incompressible flow,¹ subsonic compressible flow,^{2,3} and supersonic flow.⁴ These analyses have also been extended to three-dimensional flow.^{5,6} Unsteady aerodynamic models that consider airfoils with thickness and camber have been developed for potential flow^{7–9} and Euler flow.^{10–13}

Presented as Paper 95-2652 at the AIAA/ASME/SAE/ASEE 31st Joint Propulsion Conference and Exhibit, San Diego, CA, July 10–12, 1995; received July 28, 1995; revision received Dec. 5, 1995; accepted for publication Dec. 20, 1995. Copyright © 1995 by the American Institute of Aeronautics and Astronautics, Inc. All rights reserved.

*Assistant Professor, Department of Mechanical and Aeronautical Engineering. Member AIAA.

†Fellow, Aeromechanics and Structures and Dynamics.

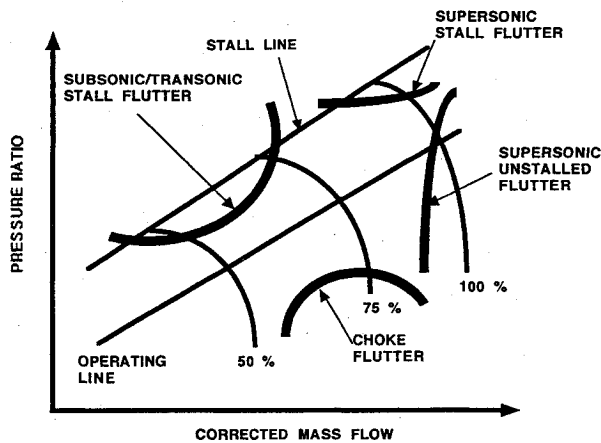


Fig. 1 Schematic of compressor performance map showing flutter boundaries.

To accurately account for viscous effects, unsteady Navier-Stokes models have been developed.¹⁴⁻¹⁶ For these Reynolds-averaged equations, turbulence models are needed for the Reynolds stress terms. Typically, the Baldwin and Lomax¹⁷ algebraic turbulence model is used for solid surfaces with turbulent wakes modeled using a turbulent wake model. Since the Reynolds numbers in turbomachinery are large enough to guarantee the flow is turbulent, suitable turbulence models are crucial for accurate prediction of steady flow performance and stall flutter assessment in fans and compressors.

Wu et al.¹⁶ have investigated the effects of the Baldwin-Lomax, Johnson-King, and $k-\epsilon$ turbulence models on steady and unsteady aerodynamic loads on a wing. The results of this study showed that for steady and unsteady attached flows, the three turbulence models gave reasonable agreement with steady and unsteady aerodynamic loads. However, for unsteady separated flow, the correlation with experiment was not adequate.

Additionally, subsonic/transonic stall flutter occurs at part speed. At these operating conditions the incidence angles can be quite large, and in many cases the computational models will not converge to a solution for the steady flow. These models are currently in the development phase. To compensate for these shortcomings, empirical and semiempirical methods are commonly used for the prediction of stall flutter by the turbomachinery designer.

In this article, stall flutter prediction techniques for fan and compressor blades will be discussed. These prediction techniques include empirical, analytical, and semiempirical methods. A semiempirical approach that uses a database of unsteady aerodynamic lift and moment correction coefficients for incidence angle and stalling effects will be outlined. This method has recently been adapted for use with a structural analysis that accounts for elastic airfoil chordline deflections. Each of the stall flutter prediction techniques will be described with particular emphasis placed on the semiempirical method. This stall flutter prediction technique will be correlated with experimentally determined aerodynamic damping data for pitching oscillations of an isolated airfoil and a rectilinear cascade of compressor airfoils. The semiempirical method will then be used for stall flutter predictions of low aspect ratio fan blades.

Stall Flutter Prediction Techniques

Stall flutter prediction systems consist primarily of two distinct approaches. The first approach is based on empirical correlations of flutter boundaries based on previous engine, and fan and compressor component testing. In the second approach unsteady aerodynamic models are coupled with a structural dynamics model to determine airfoil stability. Each of these approaches will now be discussed for stall flutter.

Empirical Techniques for Stall Flutter Prediction

Because of the difficulty in predicting the unsteady aerodynamics for separated flow, purely empirical techniques have been used extensively for the design of fan and compressor blades for many years. In this approach two of the dominant physical parameters associated with the flutter phenomena are plotted as the x and y coordinates at one spanwise location along the blade (75 and 87.5% span have been used). On this plot stable and unstable regions are identified and separated by a boundary. For stall flutter the two parameters most commonly used are incidence angle and reduced velocity. Reduced velocity, which is the inverse of k , is a measure of the unsteadiness of the flow and is an important parameter in stability analyses. The reduced velocity ($V = U/b\omega$) is defined as the inlet velocity normalized by the flutter frequency (in radians per second) and half the airfoil chord. For subsonic/transonic stall flutter, the flutter mode is typically the first torsion mode, and this frequency is used for the reduced velocity.

Since different airfoil designs will have different loading levels for the same incidence angle, incidence angle may not, in general, be the most suitable parameter for stall flutter correlations. To overcome this difficulty, a normalized incidence parameter is used, which is based on the loss bucket determined from experimental cascade performance data, rather than incidence angle. The normalized incidence is defined in Eq. (1):

$$\beta_{lf} = (\beta_{\min} - \beta_i) / (\beta_{\min} - \beta_{1L}) \quad (1)$$

This parameter relates the mean incidence (relative to the minimum loss flow angle) to an incidence at a flow angle β_{1L} , where the rate of loss increase indicates susceptibility to steady-state stall. Hence, for $\beta_{lf} = 1$, the blade is taken to be stalled.

Examples of the application of this approach for stall flutter prediction can be found in Jeffers and Meece¹⁸ and EL-Aini et al.¹⁹

The empirical technique, while valuable, does not explicitly include all of the physical parameters that influence stall flutter. For this reason, the purely empirical approach is the most successful for fan and compressor airfoils of similar configuration. Hence, for new designs the boundaries generated from previous experience might not be applicable, resulting in a fan or compressor blade that is unstable. This results in an extensive (and expensive) redesign and retest program to eliminate stall flutter from the fan or compressor operating map.

Analytical Techniques for Stall Flutter Prediction

The second approach, which has been developed to overcome the deficiencies of the empirical approach, combines unsteady aerodynamics with structural dynamics to determine airfoil stability. In this first principles approach, a bladed-disk system is unstable when the total system damping, which is the sum of the aerodynamic and mechanical damping, becomes less than zero:

$$\delta_{\text{total}} = \delta_{\text{aero}} + \delta_{\text{mechanical}} \quad (2)$$

Since mechanical damping is always positive, instability results from the unsteady aerodynamic contribution δ_{aero} . As shown by Carta²⁰ for linear systems, the aerodynamic damping is proportional to the unsteady aerodynamic work and the average system kinetic energy during a cycle of oscillation, given as follows:

$$\delta_{\text{aero}} = -(NBW/4KE) \quad (3)$$

The success of this approach is largely dependent on the accurate prediction of the unsteady aerodynamic forces being exerted on the airfoil. The unsteady aerodynamic coefficients used to calculate these forces depend on the cascade geometry,

the steady aerodynamics, and the vibratory motion of the airfoil. For the extremely high positive incidence angles that occur during stall flutter, these coefficients should also consider dynamic stall effects. Currently, no unsteady aerodynamic model accurately accounts for all of these effects, and approximate methods are used for stall flutter predictions. The next two sections discuss two approaches, with the major emphasis placed on a semiempirical method for stall flutter prediction.

Analytical Flow Separation Models

In analytical flow separation models for stall flutter the classical linearized unsteady potential flow model has been extended to include separation regions. For this type of model the viscous effects are accounted for by specifying the flow separation position on the suction surface of each blade at a fixed and identical point. Within the separation region the unsteady pressure is assumed to be negligible compared to the attached flow region. With these assumptions unsteady separated flow is simplified to the point where a kernel function similar to unstalled flow could be developed. Such analyses have been developed.²¹⁻²⁵ These simplified models do not adequately model the physics of unsteady separated flow and require prior knowledge of the separation pattern on the airfoil surface.

Semiempirical Model

The semiempirical method is a hybrid method. It uses the unsteady aerodynamic coefficients from a classical flat plate analysis and corrects these coefficients for loading and separation effects by using a database of empirical coefficients that have been determined experimentally. The semiempirical method for stall flutter was developed for stall flutter prediction of fan and compressor blades.¹⁸ The database of empirical correction factors initially used the isolated airfoil data for unstalled and stalled flow from Halfman et al.²⁶ because of the lack of experimental data for cascades of airfoils. The airfoils used were similar to NACA 0012 airfoils, except for slight differences in the leading-edge region. Since this time these empirical coefficients have been modified and extended by using rig and engine test data.

The dominant parameters used for the construction of the empirical coefficients are the normalized incidence angle and the reduced frequency. This resulted from the initial use of the isolated airfoil data. Hence, effects from differences in the interblade phase angle are accounted for in the cascade unsteady aerodynamics model. The empirical correction coefficients were determined by normalizing the experimentally determined unsteady aerodynamic coefficients by their respective theoretical values (determined from Theodorsen²⁷). From this normalization process both a magnitude and phase of the empirical correction coefficients were determined as illustrated:

$$C_{\text{ratio}} = C_{\text{experiment}} / C_{\text{theory}} \quad (4)$$

$$\Delta\Phi = \Phi_{\text{experiment}} - \Phi_{\text{theory}} \quad (5)$$

These correction coefficients are determined for the unsteady aerodynamic lift and moment caused by translation (bending), and the unsteady aerodynamic lift and moment caused by pitching (torsion). Figure 2 illustrates the phase correction $\Delta\Phi$ trend for one of the unsteady aerodynamic coefficients. Notice that radical changes from the unstalled theory occur with increasing incidence indicating the effect of stalling on the unsteady aerodynamic coefficients. Similar effects occur on the other empirical coefficients.

The use of these correction coefficients means that an isolated/cascade airfoil analogy needs to be made in which the unsteady aerodynamic changes induced by incidence and flow separation are assumed to be equivalent for both an isolated airfoil and a cascade of airfoils. Based on this analogy a semiempirical method was created that modifies the unsteady aero-

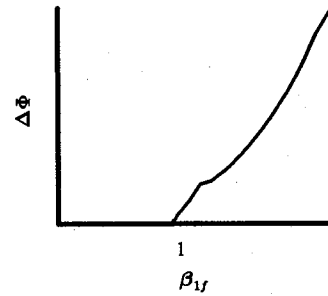


Fig. 2 Trend of phase angle correction coefficient $\Delta\Phi$ for one of the unsteady aerodynamic coefficients.

dynamic coefficients from an unstalled compressible flow theory with the empirically determined correction coefficients (amplitude ratios and phase-angle differences) from the isolated airfoil data. The unstalled cascade unsteady aerodynamic model developed by Smith² is used for the semiempirical method. Hence, for airfoil cascades, the unsteady aerodynamic coefficients from the unstalled analysis are modified:

$$C_{\text{modified}} = C_{\text{Smith}} \times C_{\text{ratio}} \quad (6)$$

$$\Phi_{\text{modified}} = \Phi_{\text{Smith}} + \Delta\Phi \quad (7)$$

The correction coefficients are used over the full incidence angle range (in terms of β_{1f}) to simulate partially and fully stalled airfoils. This permits the prediction of subsonic stall flutter using the previously discussed energy method. The semiempirical method has been used to successfully predict the flutter of high aspect ratio fan blades.¹⁹

Recently, the semiempirical method was extended for stall flutter predictions of low aspect ratio blades. The semiempirical method had been previously used for beam modes where the vibratory deflection is specified as a rigid body translation and rotation, which is directly applicable to the form of the original experimental data. For low aspect ratio blades, finite element codes are used to accurately predict the frequency and modal displacements of the bladed-disk system that may have some elastic deformation of the chordline. Hence, the vibratory deflections are specified as a displacement at each grid point on the blade surface. Since the correction coefficient database had been modified from its original form, it was desired to preserve the current form of the database. To accomplish this the vibratory displacements for the finite element analysis were decomposed into various mode functions with respect to the elastic axis of the airfoil section. This decomposition is illustrated:

$$q(\xi) = h + \alpha(\xi - \eta) + \text{higher-order polynomials} \quad (8)$$

The elastic axis position η was taken to be the shear center of the airfoil section. The database of empirical coefficients is then used to modify the translational and rotational components of the work-per-cycle for the aerodynamic damping prediction. The higher-order polynomials are not corrected for loading and stalling effects, but are included in the damping calculation. For the lower-order modes like first bending and first torsion, which are the typical stall flutter modes, this approach, as will be illustrated, was found to be acceptable.

Additionally, a transfer function was introduced to obtain the unsteady pressure distribution from the corrected unsteady lift and moment coefficients for the translation h and the rotation α components. The determination of a pressure distribution from section coefficients had previously been reported by Weiseman.²⁸ A linear transfer function is used, which is defined in Eq. (9):

$$T(\xi) = a + b(\xi - \eta) \quad (9)$$

The modified pressure distribution is formed by multiplying the transfer function by the analytical pressure distribution

$$\Delta C_{p\text{ modified}}(\xi) = T(\xi)\Delta C_{p\text{ Smith}}(\xi) \quad (10)$$

Integration of the modified pressure distribution $\Delta C_{p\text{ modified}}(\xi)$ should yield the modified lift and moment coefficients. Hence,

$$C_{L\text{ modified}} = \int T(\xi)\Delta C_{p\text{ Smith}}(\xi) d\xi \quad (11)$$

$$C_{M\text{ modified}} = \int T(\xi)(\xi - \eta)\Delta C_{p\text{ Smith}}(\xi) d\xi \quad (12)$$

where the integration limits extend over the airfoil chord. Simplifying these relationships results in two equations with the two unknown constants a and b , which can be easily determined using Cramer's rule, for example. This procedure can be utilized for both translational and rotational motions.

Note at this point that this approach suffers the same deficiencies as the empirical method, in that the database needs to be continually updated to account for new advanced airfoil designs.

Results

The modified semiempirical method will be evaluated in two parts. The first part will compare the predicted aerodynamic damping with experimental data for pitching mode oscillations of an isolated airfoil and a compressor airfoil cascade over a range of incidence angles that includes stalled flow. In the second part, stall flutter predictions are made for a wide-chord low aspect ratio fan blade. The predicted aerodynamic damping is compared with rig test results.

Isolated Airfoil Unsteady Aerodynamics

For this part of the study the isolated airfoil experimental data of Carta and Lorber²⁹ were utilized. In this experimental investigation a Sikorsky SC1095 airfoil was oscillated in pitch about the quarter-chord location at three different oscillation amplitudes at reduced frequencies up to 0.16. The oscillation amplitudes were 0.5, 2.0, and 4.0 deg. From a chordwise distribution of unsteady surface pressure measurements, the aerodynamic damping was determined and presented as a function of incidence angle and oscillation amplitude. This airfoil was found to have a steady-state stall incidence of approximately 9.5 deg. These aerodynamic damping measurements were correlated with the semiempirical method aerodynamic damping predictions for oscillation amplitudes of 0.5 and 4.0 deg. The large oscillation amplitude was of interest since the original data from Halfman et al.²⁶ used to construct the semiempirical database had a large oscillation amplitude.

Figure 3 presents the correlation of the experimentally determined aerodynamic damping for a 0.5-deg oscillation amplitude with the predicted values from the semiempirical method for incidence angles from 8 to 10.5 deg. For this correlation β_V was taken to be the incidence angle normalized by the stalling incidence angle. The isolated airfoil unstalled unsteady aerodynamic coefficients were obtained by using Theodorsen's model in place of Smith's cascade model.

Two solutions are presented for the semiempirical predictions. Each solution corresponds to a different number of airfoil collocation points. The first solution is for 10 points and the second for 20 points, and the predicted aerodynamic damping is identical for each discretization. In this study 20 airfoil collocation points were used for all calculations. For the low-to-moderate reduced frequencies considered in this investigation this was found to be more than adequate.

A number of striking features are apparent in this figure. First, rapid changes in the aerodynamic damping are exhibited

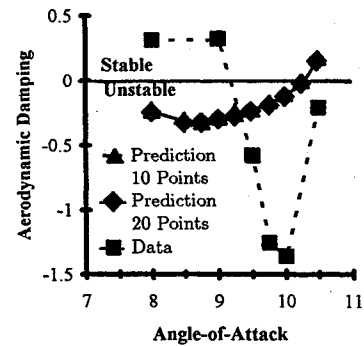


Fig. 3 Correlation of the semiempirical method aerodynamic damping predictions with experimental data for pitching oscillations at an amplitude of 0.5 deg for an isolated airfoil.

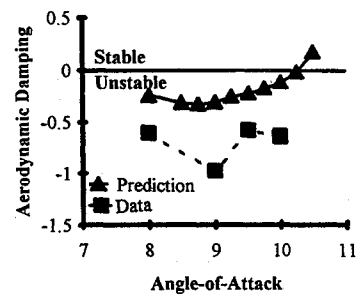


Fig. 4 Correlation of the semiempirical method aerodynamic damping predictions with experimental data for pitching oscillations at an amplitude of 4.0 deg for an isolated airfoil.

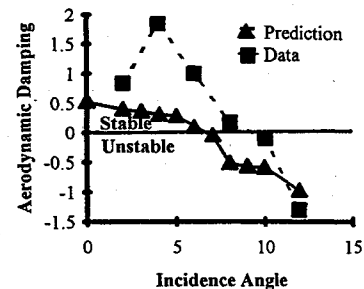


Fig. 5 Correlation of the semiempirical method aerodynamic damping predictions with experimental data for pitching oscillation of an airfoil cascade.

by the experimental data in the vicinity of the stall point as expected. Secondly, both the predicted and experimental values of aerodynamic damping increase towards stability with increasing incidence. Additionally, the predicted aerodynamic damping values show an instability in the 8- and 9-deg range, whereas the experimental data indicate stability. In fact, the predicted aerodynamic damping becomes negative at an incidence angle of 7 deg, indicating a conservative design system. However, the predicted aerodynamic damping values are larger for incidence angles larger than 9.5 deg, with the predicted values becoming positive for incidence angles greater than 10.5 deg. While the experimental data are also showing this same trend, the experiment still indicates instability.

At an oscillation amplitude of 4.0 deg, the experimental damping was also found to always be negative in the range of mean incidence angles studied, as illustrated in Fig. 4. This indicates, not surprisingly, the importance of pitching amplitude on unsteady aerodynamics in the stall region. The predicted aerodynamic damping is seen to have good trendwise agreement with the experimental data.

Cascade Unsteady Aerodynamics

Figure 5 illustrates the aerodynamic damping vs incidence angle for a rectilinear compressor cascade of airfoils. The cas-

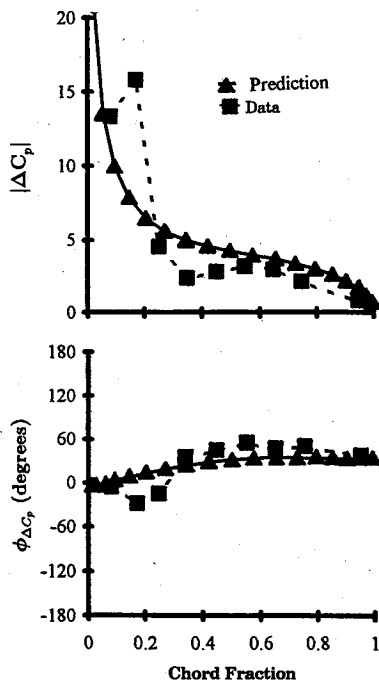


Fig. 6 Correlation of the semiempirical method unsteady aerodynamic pressure difference coefficient with experimental data for pitching oscillations of an airfoil cascade.

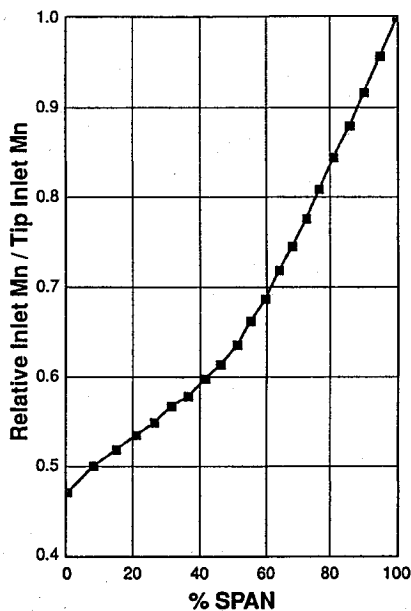


Fig. 7 Wide-chord fan blade leading-edge relative Mach number for semiempirical method stall flutter analysis.

cade results are from the Fifth Standard Configuration presented by Böls and Fransson.³⁰ These symmetric airfoils had a stagger angle of 59.3 deg with a thickness-to-chord ratio of 0.027. Experimental values of aerodynamic damping are presented for incidence angles up to 12 deg, with an inlet Mach number of 0.5, a reduced frequency of 0.37, and steady-state stall of approximately 7.9 deg. The loss correlation system was used to determine the values of β_{1f} . Chordwise pressure distributions of the unsteady surface pressure were only presented for incidence angles up to 6 deg. In this cascade experiment only one airfoil was oscillated in pitch. Hence, the infinite cascade unsteady aerodynamic coefficients were transformed to influence coefficient form using the technique presented by Buffum and Fleeter³¹ to obtain the predicted aerodynamic damping for one airfoil oscillating in an infinite cascade.

The predicted values of the aerodynamic damping decrease with increasing incidence angle and indicate an instability for incidence angles greater than 7 deg, whereas the experimental data indicate instability for incidence angles greater than 8 deg. In general, the semiempirical method predicts less stable damping values than the experiment. However, the predicted values of the damping have excellent trendwise agreement with the experimental data and indicate conservatism.

Using the transfer function, the unsteady pressure difference coefficient was also predicted by the semiempirical method and is depicted in Fig. 6 for an incidence angle of 6 deg. The data/theory correlation is presented in the form of a magnitude and phase. There is good trendwise agreement with the experimental data, but the semiempirical method predicts a slightly higher magnitude and lower phase angle in the mid-chord region.

Wide-Chord Fan Blade Flutter Predictions

The semiempirical code has been used to correctly predict part-speed stall flutter events on wide-chord shroudless fans. The code was used in the design and development phase, in conjunction with a structural optimization code, to produce flutter-free minimum weight airfoil designs.

The first configuration is for an advanced low aspect ratio fan operating at a transonic relative inlet Mach number and

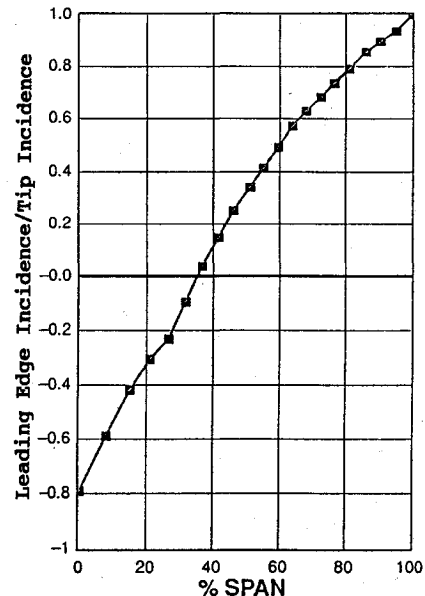


Fig. 8 Wide-chord fan blade incidence angle for semiempirical method stall flutter analysis.

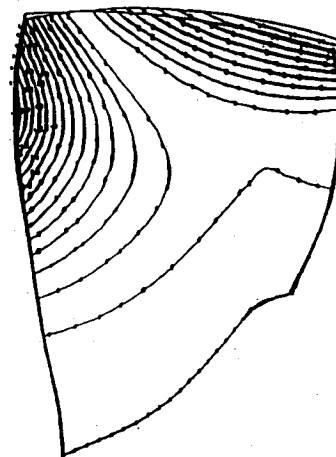


Fig. 9 Baseline blade first torsion mode shape used in semiempirical method stall flutter analysis (790 Hz).

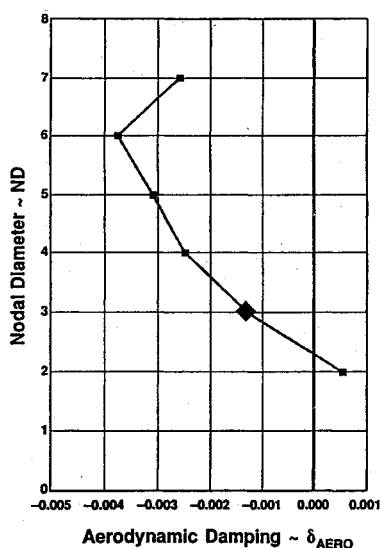


Fig. 10 Semiempirical method aerodynamic damping predictions for the wide-chord fan baseline configuration with the nozzle open.

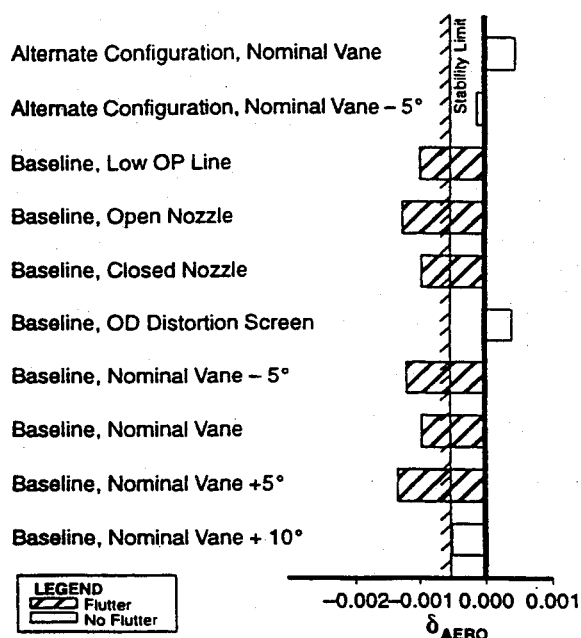


Fig. 11 First torsion mode semiempirical stall flutter predictions for low aspect ratio wide-chord fan blades.

high incidence corresponding to a simulated part-speed off-design condition. The distribution of leading-edge Mach number and incidence is shown in Figs. 7 and 8, respectively. The mode of interest, shown in Fig. 9, is the first torsion mode with a frequency of 790 Hz at the operating speed of interest. Typical aerodynamic damping predictions for a range of nodal diameters for this fan are shown in Fig. 10.

This fan exhibited nonintegral limit cycle (flutter) response in the 3-nodal pattern in a test vehicle. The semiempirical code accurately predicted the flutter events at other test conditions corresponding to different inlet conditions, including low operating line, upstream angular vane position, and distorted inlet effects. Comparison of the predicted aerodynamic damping for the 3-nodal pattern is presented in a bar chart form in Fig. 11. With the results of the nominal operating line and nominal vane position as a baseline, the code predicted the trends of all other test conditions correctly.

An alternate airfoil configuration, with nearly identical aerodynamic inlet conditions, was designed and tested under sim-

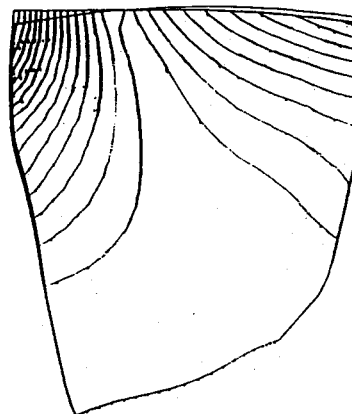


Fig. 12 Alternate blade first torsion mode used in semiempirical stall flutter analysis (820 Hz).

ilar conditions. This alternate configuration has a first torsion frequency of 820 Hz with a mode shape as shown in Fig. 12. The semiempirical code predictions, shown in Fig. 11, indicated the alternate configuration to be more stable in the 3-nodal pattern relative to the baseline configuration. When tested, this alternate configuration demonstrated significantly higher flutter margin as indicated in Fig. 11 relative to baseline.

Currently, there is a lack of appropriate unsteady cascade data in the unsteady partially and fully stalled area at transonic Mach numbers. This type of benchmark data is necessary for validation of the assumptions used in the advanced viscous analyses now under development. This type of data is also necessary for enhancement of hybrid approaches like the semiempirical method.

Conclusions

The following conclusions are based on the current state of the art of stall flutter prediction methodology and reflects the perception of turbomachinery designers:

- 1) Empirical approaches based on two- or three-parameter correlations are of limited benefit for designs that deviate from the database used to establish the boundaries separating flutter from safe operation.
- 2) Semiempirical models that combine the important structural dynamics, steady flow, and unsteady flow parameters with corrections based on experimental databases can provide more reliable trends than empirical or simplified analytical models.
- 3) Current state-of-the-art motion dependent (unsteady) computational fluid dynamic codes have not been demonstrated to provide accurate predictions for stall flutter at high incidence (10–20 deg) and transonic relative inlet Mach numbers.
- 4) Stall flutter databases that include the effects of large incidence, transonic flow, and a wide range of reduced frequencies are needed for advanced fan and compressor airfoil designs.
- 5) Efficient steady and unsteady flow solvers that incorporate realistic turbulence models need to be developed and validated for stall flutter applications.

Acknowledgment

The authors gratefully acknowledge Pratt and Whitney, Government Engines and Space Propulsion for support of this research and permission to publish this article.

References

- 1 Whitehead, D. S., "Force and Moment Coefficients for Vibrating Aerofoils in Cascade," Aeronautical Research Council Reports and Memoranda 3254, 1960.

- ²Smith, S. N., "Discrete Frequency Sound Generation in Axial Flow Turbomachines," Aeronautical Research Council Reports and Memoranda 3709, 1973.
- ³Fleeter, S., "Fluctuating Lift and Moment Coefficients for Cascaded Airfoils in a Nonuniform Compressible Flow," *Journal of Aircraft*, Vol. 10, No. 2, 1973, pp. 93-98.
- ⁴Verdon, J. M., "Further Developments in the Aerodynamic Analysis of Unsteady Supersonic Cascades, Part 1: The Unsteady Pressure Field, Part 2: Aerodynamic Response Predictions," *Journal of Engineering for Power*, Vol. 99, No. 4, 1977, pp. 509-525.
- ⁵Kodama, H., and Namba, M., "Unsteady Lifting Surface Theory for a Rotating Cascade of Swept Blades," *Journal of Turbomachinery*, Vol. 112, No. 3, 1990, pp. 411-417.
- ⁶Williams, M. H., Cho, J., and Dalton, W. N., "Unsteady Aerodynamic Analysis of Ducted Fans," *Journal of Propulsion and Power*, Vol. 7, No. 5, 1991, pp. 800-804.
- ⁷Caruthers, J. E., "Aerodynamic Analysis of Cascade Airfoils in Unsteady Rotational Flow," *Proceedings of the 2nd International Symposium on Aeroelasticity in Turbomachines*, edited by P. Suter, Juris-Verlag, Zurich, 1980, pp. 31-64.
- ⁸Verdon, J. M., and Caspar, J. R., "A Linearized Unsteady Aerodynamic Analysis for Transonic Cascades," *Journal of Fluid Mechanics*, Vol. 149, 1984, pp. 403-429.
- ⁹Whitehead, D. S., and Grant, R. J., "Force and Moment Coefficients for High Deflection Cascades," Cambridge Univ., Engineering Dept., CUED/A-Turbo/TR 98, Cambridge, England, UK, 1980.
- ¹⁰Hall, K. C., and Crawley, E. F., "Calculation of Unsteady Flows in Turbomachinery Using the Linearized Euler Equations," *Proceedings of the 4th International Symposium on Unsteady Aerodynamics and Aeroelasticity of Turbomachines and Propellers*, Aachen, Germany, 1987, pp. 15-38.
- ¹¹Gerolymos, G. A., "Numerical Integration of the 3D Unsteady Euler Equations for Flutter Analysis of Axial Flow Compressors," American Society of Mechanical Engineers Paper 88-GT-255, June 1988.
- ¹²Giles, M. B., "UNSFLO: A Numerical Method for Unsteady Inviscid Flow in Turbomachinery," Massachusetts Inst. of Technology Gas Turbine Lab. Rept. 195, Cambridge, MA, 1988.
- ¹³Hall, K. C., and Lorence, C. B., "Calculation of Three-Dimensional Unsteady Flows in Turbomachinery Using the Linearized Harmonic Euler Equations," American Society of Mechanical Engineers Paper 92-GT-136, June 1992.
- ¹⁴Swafford, T. W., Loe, D. H., Huff, D. L., Huddleston, D. H., and Reddy, T. S. R., "The Evolution of NPHASE: Euler/Navier-Stokes Computations of Unsteady Two-Dimensional Cascade Flow Fields," AIAA Paper 94-1834, June 1994.
- ¹⁵Sidén, L. D. G., "Numerical Simulation of Unsteady Viscous Compressible Flows Applied to Blade Flutter Analysis," American Society of Mechanical Engineers 91-GT-203, June 1991.
- ¹⁶Wu, J., Huff, D. L., and Sankar, L. N., "Evaluation of Three Turbulence Models for the Prediction of Steady and Unsteady Airloads," NASA TM 101413, Jan. 1989.
- ¹⁷Baldwin, B. S., and Lomax, H., "Thin Layer Approximation and Algebraic Model for Separated Turbulent Flows," AIAA Paper 78-257, Jan. 1978.
- ¹⁸Jeffers, J. D., II, and Meece, C. E., "F100 Fan Stall Flutter Problem Review and Solution," *Journal of Aircraft*, Vol. 12, No. 4, Jan. 1975, pp. 350-357.
- ¹⁹EL-Aini, Y. M., Bankhead, H. R., and Meece, C. E., "Subsonic/Transonic Stall Flutter Investigation of an Advanced Low Pressure Compressor," American Society of Mechanical Engineers Paper 86-GT-90, June 1986.
- ²⁰Carta, F. O., "Coupled Blade-Disk-Shroud Flutter Instabilities in Turbojet Engine Rotors," *Journal of Engineering for Power*, 1967, pp. 419-426.
- ²¹Woods, L. C., "Aerodynamic Forces on an Oscillating Aerofoil Fitted with a Spoiler," *Proceedings of the Royal Society of London, Series A: Mathematical and Physical Sciences*, No. 239, 1957, pp. 328-337.
- ²²Kelley, H. R., "An Extension of the Woods Theory for Unsteady Cavity Flows," *Journal of Basic Engineering*, Vol. 89, No. 4, 1967, pp. 789-806.
- ²³Sisto, F., "Linearized Theory of Nonstationary Cascades at Fully Stalled or Supercavitated Conditions," *ZAMM*, Vol. 47, No. 8, 1967, pp. 531-542.
- ²⁴Chi, R. M., "Separated Flow Unsteady Aerodynamic Theory," *Journal of Aircraft*, Vol. 22, No. 11, 1985, pp. 965-974.
- ²⁵Eley, J. A., and Fleeter, S., "Prediction of Airfoil Separated Flow Unsteady Aerodynamics," *International Journal of Turbo and Jet Engines*, Vol. 8, Nos. 3-4, 1991, pp. 185-210.
- ²⁶Halfman, R. L., Johnson, H. C., and Haley, S. M., "Evaluation of High Angle-of-Attack Aerodynamic Derivative Data and Stall Flutter Prediction Techniques," NACA TN 2533, 1951.
- ²⁷Theodorsen, T., "General Theory of Aerodynamic Instability and Mechanism of Flutter," NACA Rept. 496, 1935.
- ²⁸Wieseman, C. D., "Methodology for Using Steady Experimental Aerodynamic Data to Improve Steady and Unsteady Aerodynamic Analysis," M.S. Thesis, George Washington Univ., Washington, DC, 1989.
- ²⁹Carta, F. O., and Lorber, P. F., "Experimental Study of the Aerodynamics of Incipient Torsional Stall Flutter," *Journal of Propulsion and Power*, Vol. 3, No. 4, 1986, pp. 164-170.
- ³⁰Bölcs, A., and Fransson, T. H., "Aeroelasticity in Turbomachines: Comparison of Theoretical and Experimental Cascade Results," *Communication de Laboratoire de Thermique Appliquée et de Turbomachines*, No. 1, Ecole Polytechnique Fédérale de Lausanne, Switzerland, 1986.
- ³¹Buffum, D. H., and Fleeter, S., "Wind Tunnel Wall Effects in a Linear Oscillating Cascade," *Journal of Turbomachinery*, Vol. 115, No. 1, 1993, pp. 147-156.